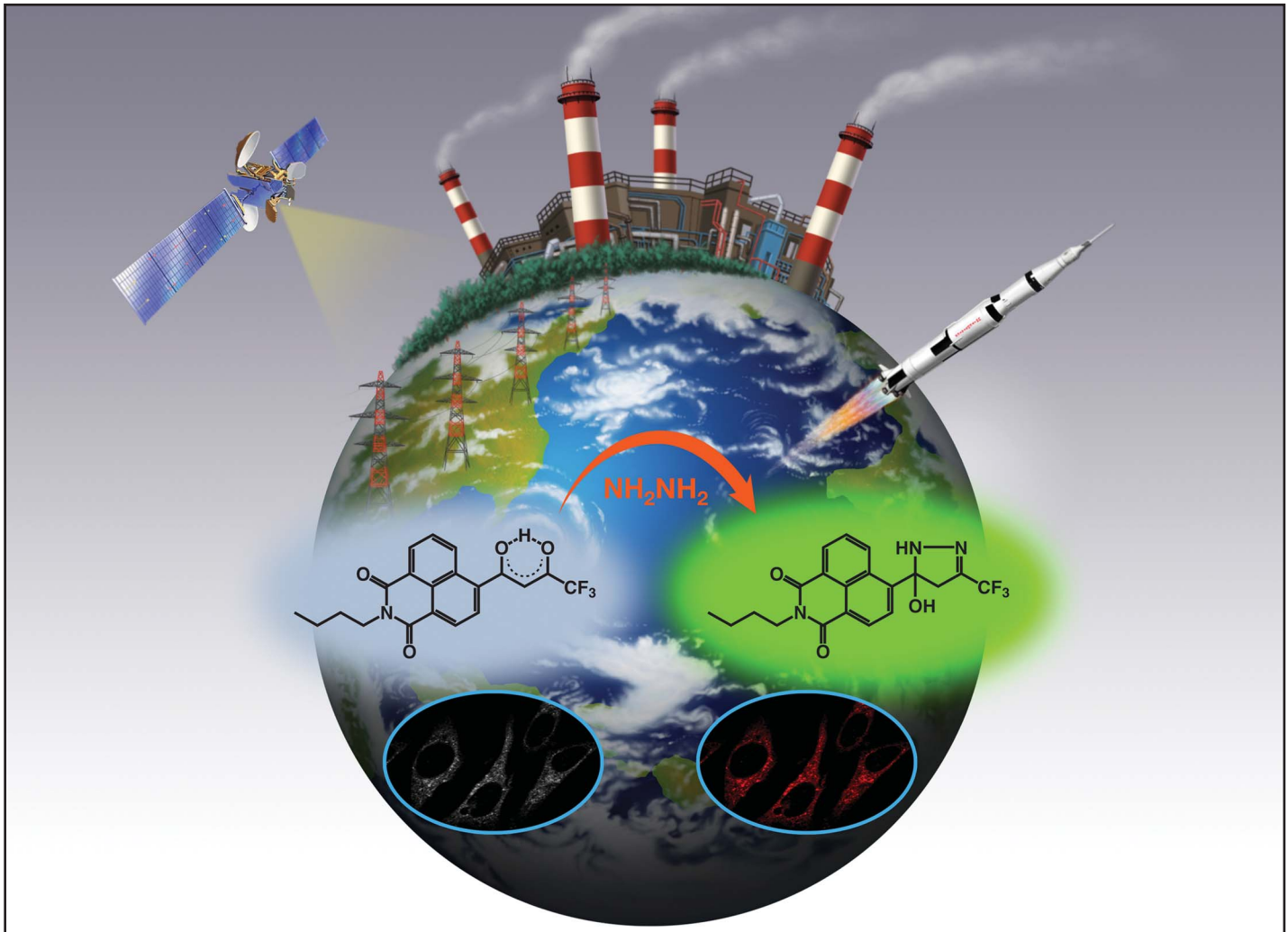

Showcasing work from the laboratories of Prof. Jonathan L. Sessler and Prof. Jong Seung Kim at the University of Texas at Austin, Texas, USA and Korea University, Seoul, Korea.

Naphthalimide trifluoroacetyl acetonate: a hydrazine-selective chemodosimetric sensor

A trifluoroacetyl acetonate naphthalimide derivative was synthesized in good yield and reacts selectively with hydrazine to give a five-membered ring. This leads to OFF–ON fluorescence with a maximum intensity at 501 nm as well as easily discernible color changes.

As featured in:

See Jong Seung Kim and Jonathan L. Sessler *et al.*, *Chem. Sci.*, 2013, **4**, 4121.

RSC Publishing

www.rsc.org/chemicalscience

Registered Charity Number 207890

Chemical Science

RSC Publishing

EDGE ARTICLE

View Article Online
View Journal | View Issue

Cite this: *Chem. Sci.*, 2013, **4**, 4121

Naphthalimide trifluoroacetyl acetonate: a hydrazine-selective chemodosimetric sensor†

Min Hee Lee,[a] Byungkwon Yoon,[b] Jong Seung Kim*[b] and Jonathan L. Sessler*[ac]

Received 28th June 2013
Accepted 13th August 2013

DOI: 10.1039/c3sc51813b

www.rsc.org/chemicalscience

The trifluoroacetyl acetonate naphthalimide derivative **1** has been synthesized in good yield. In acetonitrile solution, compound **1** reacts selectively with hydrazine (NH_2NH_2) to give a five-membered ring. This leads to OFF–ON fluorescence with a maximum intensity at 501 nm as well as easily discernible color changes. Based on a readily discernible and reproducible 3.9% change in overall fluorescence intensity, the limit of detection for **1** is 3.2 ppb (0.1 μM), which is below the accepted limit for hydrazine set by the U.S. Environmental Protection Agency (EPA). Compound **1** is selective for hydrazine over other amines, including NH_4OH, NH_2OH, ethylenediamine, methylamine, *n*-butylamine, piperazine, dimethylamine, triethylamine, pyridine, and is not perturbed by environmentally abundant metal ions. When supported on glass-backed silica gel TLC plates, compound **1** acts as a fluorimetric and colorimetric probe for hydrazine vapor at a partial pressure of 9.0 mm Hg, with selectivity over other potentially interfering volatile analytes, including ammonia, methylamine, *n*-butylamine, formaldehyde, acetaldehyde, H_2O_2, HCl, and CO_2 being observed. Probe **1** can also be used for the detection of hydrazine in HeLa cells and does so without appreciable interference from other biologically abundant amines and metal ions.

Introduction

Sensor systems that might allow for the effective and rapid detection of analytes constitute a major current focus in green chemistry.[1] New analytical tools are needed for real-time industrial process monitoring and for preventing the formation of toxic materials. Such monitoring allows for the rapid detection of toxic materials, thus minimizing errors while providing potential cost reductions relative to traditional laboratory-based analyses. In this context, fluorescent probes have long been of particular interest to analytical scientists. Recently, a number of fluorescent probes have been put forward for the detection of anions,[2] metal ions,[3] and cellular components,[4] *etc.*

Hydrazine is of particular interest given its toxicity and high levels of use. It is used as a blowing agent for the production of plastics, as a gas-forming agent in air bags, in agricultural chemicals and preservatives, and is found in tobacco.[5,6] It is also used as an antioxidant in nuclear and in electrical power plants, as an anti-corrosion agent, and as a fuel for satellites and rockets.[7] Additionally, it was reported that some nitrogen fixing bacteria may create hydrazine as a by-product.[8] Exposure to hydrazine is known to cause critical damage to the liver, kidney, and central nervous system in humans.[9] Hydrazine has been classified as a probable human carcinogen by the U.S. Environmental Protection Agency (EPA), which has set an exposure limit of 10 ppb.[10] This has provided an incentive to develop new methods for the detection of hydrazine.

To date, a variety of analytical techniques, including chromatography-mass spectrometric,[6,11] titrimetric,[12] and electrochemical methods have been exploited for the purpose of hydrazine analysis.[13] However, there are only a few reports regarding fluorescent probes. Swager *et al.* reported a fluorescent polymer that is reduced by hydrazine vapor, giving rise to an increase in fluorescence intensity.[14] Chang *et al.* developed a fluorescence turn-on type probe for hydrazine by deprotection of levulinoyl ester or acetyl groups.[15] Fan *et al.* reported a ratiometric fluorescent probe based on the reaction of hydrazine with arylidenemalononitrile.[16] In addition, Tong *et al.* reported that arylaldehydes react with hydrazine to produce a fluorescent product.[17] However, there is still a question concerning the selective detection of hydrazine over other competitive amines such as ammonia, diamines and alkylamines. A particular challenge is to develop hydrazine probes that are biocompatible and which could be used in cellular milieus since this might allow toxic events to be monitored in real time and the biological effects of hydrazine to be studied in greater detail under controlled *in vitro* conditions. Herein, we report a new fluorescent probe **1** capable of selectively sensing

[a]*Department of Chemistry and Biochemistry, The University of Texas at Austin, Austin, TX 78712-1224, USA*

[b]*Department of Chemistry, Korea University, Seoul 136-701, Korea. E-mail: jongskim@korea.ac.kr; Fax: +82-2-3290-3121*

[c]*Department of Chemistry, Yonsei University, Seoul 120-749, Korea. E-mail: sessler@cm.utexas.edu; Fax: +82 512 471-7550*

† Electronic supplementary information (ESI) available: Experimental details, Mass and NMR spectra; X-ray crystallographic details. CCDC 942177. For ESI and crystallographic data in CIF or other electronic format see DOI: 10.1039/c3sc51813b

hydrazine over other amines with fluorescence turn-on manner and show that the system functions *inter alia* in HeLa cells.

Results and discussion

Probe **1** was prepared by the synthetic route outlined in Scheme 1. The naphthalimide derivatives **4** and **5** were synthesized by adapting published procedures.[18] Compound **6**, was obtained by reacting intermediate **5** with *n*-butylamine in ethanol. Claisen condensation of **6** with ethyl trifluoroacetate then gave probe **1** in 88% yield. The chemical structures of **1** and **6** were confirmed by ^{1}H NMR and ^{13}C NMR spectroscopy, as well as HR-FAB and ESI mass spectrometry (Fig. S18–S23†). The ^{1}H NMR spectrum of **1** is characterized by a broad –O*H* peak at 14.7 ppm and a sharp singlet –C*H* peak at 6.7 ppm, both of which correspond to the trifluoroacetyl acetonate moiety. Based on literature precedent, compound **1** is thought to exist as a mixture of enol forms as depicted in Scheme S1.†[19]

Initial spectroscopic studies of **1** were undertaken by monitoring the UV/Vis absorption and fluorescence spectral changes observed upon the addition of hydrazine and other amines in CH_3CN solution at room temperature. In the absence of hydrazine, probe **1** displays two absorption bands centered at 295 ($\varepsilon = 7.4 \times 10^3$ M^{-1} cm^{-1}) and 348 nm ($\varepsilon = 1.7 \times 10^4$ M^{-1} cm^{-1}), respectively, as well as a weak emission feature at 445 nm ($\Phi_f = 0.004$),[20] as shown in Fig. 1 and S1.† On the basis of comparisons with **6**, the absorption band at 348 nm is thought to originate with the naphthalimide moiety.

As shown in Fig. 1a, addition of hydrazine (1.0 mM) to a CH_3CN solution of **1** leads to an increase in the fluorescence intensity along with a red-shift from 445 to 501 nm. In contrast, only a fluorescence quenching at 445 nm or an insignificant change was observed upon the addition of a variety of other test amines, including ammonium hydroxide, hydroxylamine, ethylenediamine, methylamine, *n*-butylamine, piperazine, dimethylamine, triethylamine, and pyridine (1.0 mM, respectively). However, when exposed to most amines other than pyridine the absorbance feature at 348 nm was observed to decrease in intensity, whereas that at 295 nm was found to increase (Fig. S2†). Nevertheless it is important to appreciate that even when added at a 30-fold excess relative to hydrazine, no inhibition of the hydrazine-induced fluorescence response was seen (*vide infra*). The effect of environmentally abundant metal ions, such as Cs^+, Na^+, K^+, Ca^{2+}, Mg^{2+}, Zn^{2+}, Cu^{2+}, Mn^{2+}, Fe^{2+}, Fe^{3+}, Hg^{2+}, Pb^{2+}, Cd^{2+}, Ni^{2+}, and Ba^{2+} (as the chloride salts),

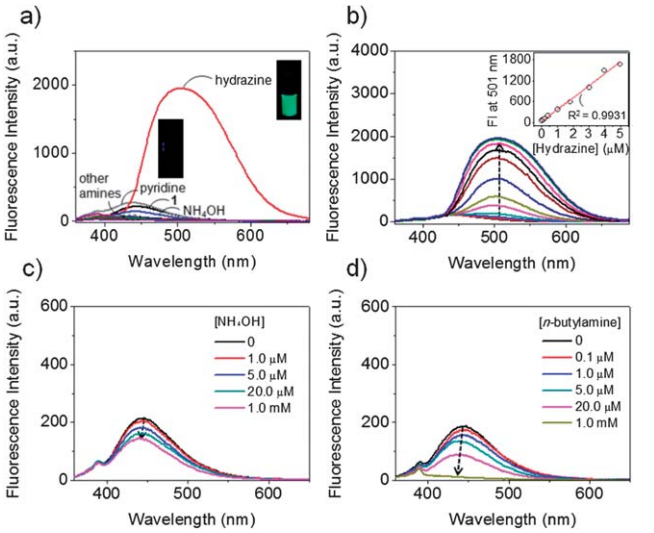

Fig. 1 (a) Fluorescence spectra of **1** (10.0 μM) recorded in the presence of various amines, including hydrazine, ammonium hydroxide (NH_4OH), hydroxylamine, ethylenediamine, methylamine, *n*-butylamine, piperazine, dimethylamine, triethylamine, and pyridine (1.0 mM, respectively). (b) Fluorescence increase observed for **1** (10.0 μM) in the presence of increasing concentrations of hydrazine (0, 0.1, 0.2, 0.4, 1.0, 1.8, 3.0, 4.0, 5.0, 6.0, 10.0, 20.0 μM). Inset: plot showing the linear relationship between the fluorescence intensity at 501 nm and the hydrazine concentration (0, 0.1, 0.2, 0.4, 1.0, 1.8, 3.0, 4.0, 5.0 μM). Fluorescence quenching observed for **1** (10.0 μM) in the presence of increasing concentrations of NH_4OH (c) and *n*-butylamine (d), respectively. All spectra were acquired 1 h after addition of the amine at room temperature in CH_3CN, with excitation effected at 348 nm.

was also tested. However, no appreciable spectroscopic changes were seen (Fig. S3†). Taken in concert, these findings lead us to suggest that **1** could be used to detect hydrazine selectively even in milieus that contain potential interferants.

The reaction of **1** with hydrazine is thought to produce a cyclized product (**2**) resulting in an increase in the intensity of the emission feature at 501 nm (Scheme 2). In contrast to what proved true for **1**, neither the absorption nor fluorescence spectral features undergo appreciable changes when **6** is exposed to hydrazine in CH_3CN (Fig. S4†). On this basis, we conclude (1) that the trifluoroacetyl acetonate unit reacts

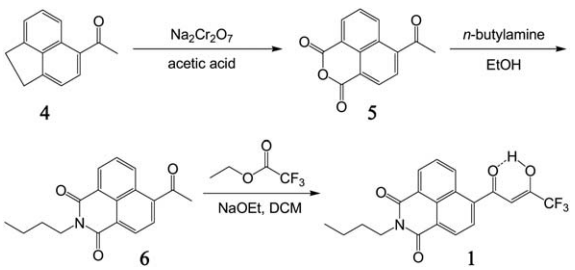

Scheme 1 Synthesis of probe **1**.

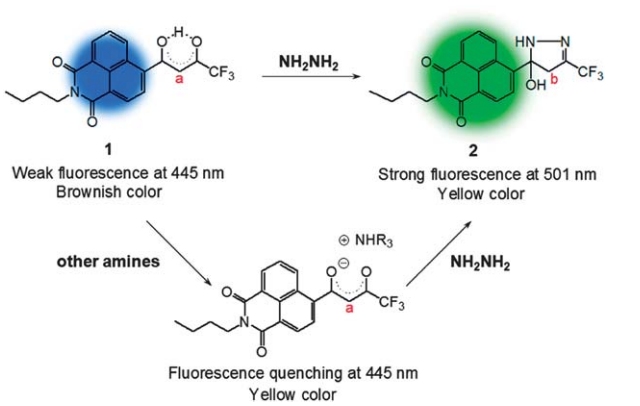

Scheme 2 Proposed reactions of **1** with hydrazine and other amines.

selectively and stoichiometrically with hydrazine, but that (2) other amines do not induce the cyclization reaction that gives rise to the observed fluorescence enhancement. The contrasting reactions with hydrazine and other amines are shown in Scheme 2 and discussed further below.

Quantitative assessments of the fluorescence spectral changes were made by treating probe **1** with increasing concentrations of hydrazine (0–20.0 μM) in CH_3CN (Fig. 1b). The fluorescence intensity at 445 nm decreases in a monotonic fashion whereas that of the feature at 501 nm increases (33-fold, $\Phi_f = 0.43$)[20] with an isosbestic point being observed at 430 nm. The response produced at any given hydrazine concentration was not instantaneous. However, at all concentrations the response occurred within one hour, with no further appreciable spectral changes taking place (see Fig. S5†). The fluorescence intensity reached a plateau upon the addition of 1.0 equiv. (10.0 μM) of hydrazine. The UV/Vis spectra of **1** with various hydrazine concentrations (0–20.0 μM) were also recorded; they are shown in Fig. S6† and reveal a pattern of ratiometric changes that matches the fluorescence behavior. A linear relationship ($R^2 = 0.9931$) was found between the emission intensity at 501 nm and the hydrazine concentration over the 0–5.0 μM range. From this linear relationship, and using a reproducible and readily discernible 3.9% change in overall fluorescence intensity as the standard, the detection limit of probe **1** for hydrazine is 0.1 μM (3.2 ppb) (*cf.* inset to Fig. 1b). On this basis we conclude that compound **1** may be used as an Off–On fluorescent signaling agent with a limit of detection that is below the 10 ppb limit for hydrazine exposure set by the U.S. EPA.[10]

To gain insight into the selectivity of probe **1** for hydrazine over other amines, the fluorescence changes of **1** in the presence of increasing concentrations of other amines were recorded in CH_3CN under conditions identical to those used for hydrazine. Fig. 1c and d are indicative of fluorescence changes seen when probe **1** is exposed to NH_4OH and *n*-butylamine, respectively. In the presence of high concentrations of these bases, the fluorescence intensity of probe **1** at 445 nm is somewhat quenched while a slight blue shift in the emission maximum is seen. This stands in sharp contrast to what is seen with hydrazine (*vide infra*).

Competition experiments were also carried out. Upon the addition of various amines (0.3 mM, respectively) to a solution of **1** (10.0 μM), fluorescence quenching was observed as demonstrated in Fig. S7.† However, when 0.3 mM of hydrazine was then added to the resulting mixtures containing **1** and the amine in question, a strong fluorescent emission at 501 nm was seen. On this basis, we conclude that probe **1** undergoes a hydrazine-induced cyclization to give a fluorescence enhancement even in the presence of other potentially competitive amines.

In Scheme 2 proposed reactions of **1** with hydrazine and other amines are shown. Proton NMR spectroscopic and ESI mass spectrometric data consistent with the structure proposed for product **2** were obtained. Fig. 2 shows the ^{1}H NMR spectrum of **1** recorded in the absence and presence of 2.0 equiv. of hydrazine, *n*-butylamine, triethylamine, dimethylamine, ammonium hydroxide, and pyridine, respectively, in CD_3CN. Upon the addition of hydrazine, the –C*H* (a) peak of the trifluoroacetyl acetonate moiety at δ 6.7 (1H) disappears.

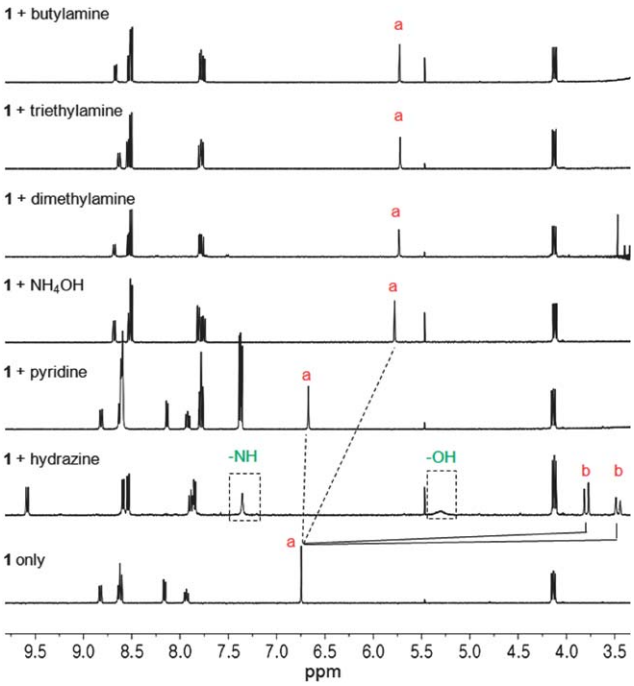

Fig. 2 Partial ^{1}H NMR spectra of **1** recorded upon the addition of 2.0 equiv. of *n*-butylamine, triethylamine, dimethylamine, ammonium hydroxide (NH_4OH), hydrazine, and pyridine, respectively, in CD_3CN.

Concurrently, two pair of doublets at δ 3.8 (1H) and 3.4 (1H), corresponding to the –CH_2 resonances (b) of the pyrazole subunit are observed. Moreover, two broad peaks at δ 7.3 (1H) and 5.3 (1H), corresponding to the –N*H* and –O*H* signals of **2**, respectively, were observed. In addition, changes in the chemical shifts for the aromatic protons of the naphthalimide core were found. On the basis of the ^{1}H NMR spectra recorded in the presence of varying concentrations of hydrazine it is concluded that only 1.0 equiv. of hydrazine is required to convert probe **1** completely into **2** (Fig. S8†). ESI-MS analyses of **2** revealed the expected fragmentation patterns and primary peaks ([**2** + H]$^+$ and [**2** + Na]$^+$, *m*/*z* 406.138 and 428.119, respectively) (Fig. S9†).

The proposed daughter product **2** was also isolated and its structure confirmed by ^{1}H NMR and ESI-MS spectroscopic analyses, as shown in Fig. S10 and S11.† Based on time dependent analyses, product **2** is found to be quite stable in CD_3CN over the course of several days (Fig. S12†). Interestingly, in $CDCl_3$, as opposed to CD_3CN, compound **2** proved unstable; it undergoes dehydration to give a crystalline product **3** whose identity was confirmed by ^{1}H NMR, ESI-MS, and X-ray crystallographic analyses (Fig. S13, S24, and Tables S1–S7†). This solvent dependent behavior is ascribed to the fact that $CHCl_3$ can decompose, especially under UV light, to produce H^+, which can trigger the proposed dehydration reaction that serves to produce **3** from **2**.[21]

In contrast to what is seen with hydrazine, the addition of other amines, including *n*-butylamine, triethylamine, dimethylamine, and ammonium hydroxide, to probe **1** causes the –C*H* (a) to shift to higher field (from δ 6.7 to 5.7). The ^{1}H NMR spectra of *n*-butylamine, dimethylamine, and triethylamine

were also recorded in the absence and presence of **1** in CD_3CN. Upon the addition of **1**, the alkyl protons of the amines were found to shift to lower field as shown in Fig. S14–S16.† However, in the case of pyridine, a negligible change was observed probably due to its weak basicity. These results lead us to propose that the amines deprotonate the acidic –O*H* proton within the trifluoroacetyl acetonate moiety of **1** leading to a quenching of the fluorescence signal at 445 nm as depicted in Scheme 2.

Next, we investigated whether **1** displays a hydrazine-dependent change in its fluorescence signature when used in aqueous environments. Toward this end, probe **1** was exposed to a 1.0 mM solution of hydrazine in a mixture of H_2O–CH_3CN (v/v, 1 : 9). Under these conditions, a new emission band, presumably induced by the cyclization reaction of **1** with hydrazine, was observed at 534 nm as shown in Fig. 3. We also monitored the changes in the fluorescence intensity at 534 nm when probe **1** was treated with increasing concentrations of hydrazine. The fluorescence intensity increases by approximately 3-fold with good linearity with respect to [hydrazine] being seen over a wide concentration range (0–10.0 μM) (R^2 = 0.99, Fig. 3b). On this basis we conclude that probe **1** is capable of detecting hydrazine both in mixed aqueous-organic environments.

The pH dependence of the hydrazine-induced cyclization reaction was also investigated. As seen in Fig. S17,† probe **1** is stable over a pH range of 2 to 12. On the other hand, it readily reacts with hydrazine within a pH range of 2 to 5. Such findings led us to consider that **1** may be used to detect hydrazine effectively in acidic environments.

We also tested whether probe **1** would react with hydrazine gas or other vaporized organic materials (*i.e.*, formaldehyde, acetaldehyde, H_2O_2, HCl, CO_2, ammonia, methylamine, and *n*-butylamine). For these tests, glass TLC plates were soaked in a CH_3CN solution of **1** (5.0 mM) and dried. The TLC plates coated with **1** were then exposed to vapors of each sample for 1.0 min, respectively. This was done under conditions where the vapors were in considerable excess relative to **1**. As shown in Fig. 4, upon exposure of hydrazine vapor at a partial pressure of 9.0 mm Hg, distinctive changes were observed in the fluorescence (from blue to green) and color (from white gray to yellow) of the TLC plates. While in the case of other amines a visual color change from white gray to yellow is seen, the change in the fluorescent is negligible. Moreover, no detectable changes or trace differences were observed upon exposure of probe **1** to other environmentally abundant vapors, such as formaldehyde, acetaldehyde, H_2O_2, HCl, and CO_2. Again, these findings provide support for the contention that **1** can selectively detect hydrazine vapor as the result of a specific cyclization reaction that gives rise to fluorescent and visual color changes that are detectable both in solution and when the probe is present on the surface of a TLC plate.

We also examined whether **1** can be used for the detection of hydrazine in cells. In this study, HeLa cells were incubated with probe **1** and then separately treated with various concentrations of hydrazine (0, 0.1, 0.5 and 1.0 mM). Fluorescence images were then acquired *via* confocal microscopy. As shown in Fig. 5, upon two-photon excitation at 740 nm, probe **1** displays a strong fluorescence signature in the presence of hydrazine. Moreover, the fluorescence intensity of **1** in HeLa cells was seen to depend on the concentration of hydrazine in the cellular medium.

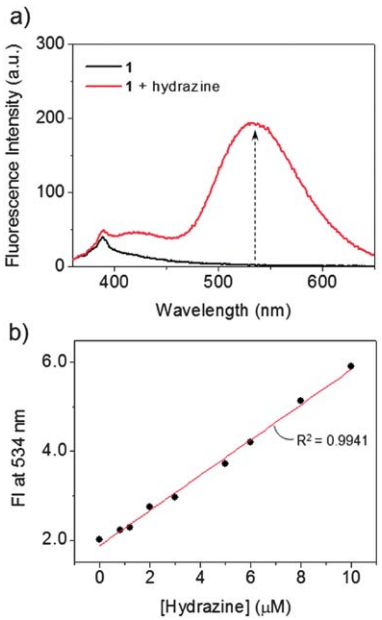

Fig. 3 (a) Fluorescence spectra of **1** (10.0 μM) recorded without and with hydrazine (1.0 mM) in an aqueous mixture (H_2O/CH_3CN = v/v, 1 : 9). (b) The changes in the fluorescence intensity (FI) at 534 nm observed for **1** (10.0 μM in H_2O/CH_3CN = v/v, 1 : 9) as a function of hydrazine concentration (0, 0.8, 1.2, 2.0, 3.0, 5.0, 6.0, 8.0, 10.0 μM). All spectra were acquired 1 h after hydrazine addition and obtained using excitation at 348 nm.

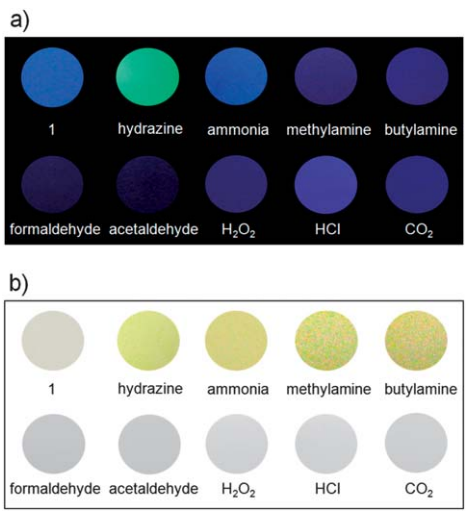

Fig. 4 (a) Fluorescent and (b) visual color changes of probe **1** (5.0 mM)-coated TLC plates after exposure to an excess quantity of various vapors, including hydrazine, ammonia, methylamine, *n*-butylamine, formaldehyde, acetaldehyde, H_2O_2, HCl, and CO_2 for 1.0 min, respectively. The fluorescent color changes were observed using a hand-held UV lamp producing an excitation at 365 nm. In the specific case of hydrazine a partial pressure of 9.0 mm Hg was used by exposing the TLC plate directly to the equilibrated head space of a 20.7 M (65%) solution of hydrazine hydrate.

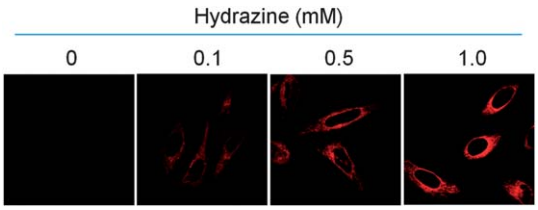

Fig. 5 Confocal microscopic images of HeLa cells treated with **1**. Cells were incubated with **1** (10.0 μM) and separately incubated with media containing hydrazine (0, 0.1, 0.5 and 1.0 mM) for 2 h at 37 °C. Fluorescence images were obtained using a two-photon excitation wavelength of 740 nm and emission wavelengths of 400–600 nm.

These results lend further support to the inference that the hydrazine-induced cyclization of **1** to produce the fluorescent species **2** is very selective and is not subject to appreciable interference from other biologically abundant amines and metal ions.

Conclusions

Compound **1**, containing a naphthalimide and bearing a trifluoroacetyl acetonate moiety for hydrazine sensing, was synthesized. This probe undergoes a selective hydrazine-induced cyclization to give a fluorescent species **2**. This results in a turn-on of the fluorescence emission signal at 501 nm and color changes within the time course of 60 min. The detection limit of **1** was found to be 3.2 ppb, which falls below the 10 ppb limit for hydrazine exposure set by the U.S. EPA. Competition experiments were carried out and served to confirm that probe **1** selectively reacts with hydrazine, even in the presence of other test amines. When coated on silica gel TLC plates, probe **1** can be used to detect vaporized hydrazine selectively as inferred from the easy-to-visualize fluorescent and color changes. Finally, it was found that probe **1** may be used to detect hydrazine in HeLa cells without appreciable interference from other biologically abundant amines or metal ions. We thus propose that probe **1** and structurally related species that exploit a selective ring-forming reaction could be used to sense hydrazine in a range of environments.

Experimental section

1 Synthetic materials and methods

All reagents, including amines, metal ions, and other chemicals for synthesis, were purchased from Aldrich, TCI and used as received. All solvents were HPLC reagent grade, and triple-deionized water was used throughout the analytical experiments. Silica gel 60 (Sorbent, 40–63 mm) was used for column chromatography. Analytical thin layer chromatography was performed using Silicycle 60 F254 silica gel (precoated sheets, 0.25 mm thick). ^{1}H and ^{13}C NMR spectra were recorded in $CDCl_3$ (Cambridge Isotope Laboratories, Cambridge, MA) on Varian 400 MHz spectrometers.

2 UV/Vis absorption and fluorescence spectroscopy

Stock solutions of compounds **1**, **6**, and amines were prepared in CH_3CN. The chloride salts of the test metal ions Cs^+, Na^+, K^+, Ca^{2+}, Mg^{2+}, Zn^{2+}, Cu^{2+}, Mn^{2+}, Fe^{2+}, Fe^{3+}, Hg^{2+}, Pb^{2+}, Cd^{2+}, Ni^{2+}, and Ba^{2+} were prepared in triple-distilled water. The fluorescence quantum yields (Φ_f) were measured relative to quinine sulfate ($\Phi_f = 0.54$ in 0.5 M H_2SO_4).[20] Absorption spectra were recorded on Varian-5000 UV/Vis-NIR spectrophotometer, and fluorescence spectra were recorded using a FL3-11T spectrofluorometer (Nanolog) equipped with a xenon lamp (FL 1039). Samples for absorption and emission measurements were contained in quartz cuvettes (3 mL volume). Excitation was provided at 348 nm with excitation and emission slit widths both set at 5 nm.

3 Cell culture and imaging

A human cervical cancer cell line (HeLa) was cultured in Dulbecco's Modified Eagle's Medium (DMEM) supplemented with 10% FBS (WelGene), penicillin (100 units per mL), and streptomycin (100 μg mL^{-1}). Two days before imaging, the cells were passed and plated on glass-bottomed dishes (MatTek). All the cells were maintained in a humidified atmosphere of 5/95 (v/v) of CO_2/air at 37 °C. For labelling, the growth medium was removed and replaced with DMEM without FBS. The cells were treated and incubated with 10 μM of **1** at 37 °C under 5% CO_2 for 2 h. The cells were washed three times with phosphate buffered saline (PBS, Gibco) and then cell images were obtained using a confocal microscope from Leica (Leica TCS SP2 model). Other information is available in the figure captions.

4 Two-photon fluorescence microscopy

Two-photon fluorescence microscopy images of HeLa cells incubated with **1** were obtained using spectral confocal and multiphoton microscopes (Leica TCS SP2 model) with a ×10 (NA = 0.30 DRY) and ×100 (NA = 1.30 OIL) objective lens. The two-photon fluorescence microscopic images were obtained using a DM IRE2 Microscope (Leica) by exciting probe **1** with a mode-locked titanium sapphire laser source (Coherent Chameleon, 90 MHz, 200 fs) set at wavelength 740 nm and using an output power of 1580 mW, which corresponded to approximately 10 mW average power in the focal plane. To obtain images, internal photomultiplier tubes (PMTs) were used to collect the signals in an 8 bit unsigned 512 × 512 pixels at 400 Hz scan speed.

5 Synthesis

Compounds **4** and **5** were prepared by adapting published procedures.[18]

Synthesis of 6. Compound **5** (2.0 g, 8.3 mmol) and *n*-butylamine (1.2 mL, 16.6 mmol) were dissolved in ethanol (100 mL). The reaction mixture was then stirred and heated at reflux for 3 h. After removal of solvent under reduced pressure, the crude product was purified over silica gel using ethyl acetate–hexanes (v/v, 1 : 2) as the eluent to yield **6** as a white solid (2.0 g, 81%). HRESI-MS m/z ($[M + Na]^+$) calc. 318.11006, obs 318.11015. ^{1}H

NMR ($CDCl_3$, 400 MHz): δ 8.91 (d, 1H, $J = 8.8$ Hz); 8.59 (d, 2H, $J = 8.6$ Hz); 8.08 (d, 1H, $J = 8.1$ Hz); 7.78 (t, 1H, $J = 7.8$ Hz); 4.12 (t, 2H, $J = 4.2$ Hz); 2.76 (s, 3H); 1.70–1.63 (m, 2H); 1.42–1.37 (m, 2H); 0.92 (t, 3H, $J = 0.9$ Hz). ^{13}C NMR ($CDCl_3$, 100 MHz): 200.6, 163.8, 163.3, 139.7, 132.3, 131.5, 129.6, 128.8, 128.3, 125.6, 122.3, 40.4, 30.3, 20.4, 14.2 ppm.

Synthesis of 1. To a solution of **6** (1.3 g, 4.4 mmol) in dichloromethane was added ethyl trifluoroacetate (10 mL). The mixture was stirred for 5 min before an ethanolic 21% NaOEt solution (20 mL) was added. The reaction mixture was then heated at reflux for 2 h under a nitrogen atmosphere in the dark. After allowing the vessel to cool to room temperature, the reaction was quenched by adding dilute $HCl_{(aq.)}$. The solution was then extracted with dichloromethane several times. The combined organic phases were dried over Na_2SO_4, and filtered. After removal of solvent under reduced pressure, the crude product was purified over silica gel using ethyl acetate–hexanes (v/v, 4 : 1) as the eluent to yield **1** as a brownish solid (1.2 g, 88%). HRESI-MS m/z ($[M + Na]^+$) calc. 414.09236, obs 414.09219. ^{1}H NMR ($CDCl_3$, 400 MHz): δ 14.8 (s, 1H); 8.79 (d, 1H, $J = 8.8$ Hz); 8.70–8.65 (m, 2H); 8.06 (d, 1H, $J = 8.1$ Hz); 7.88 (t, 1H, $J = 7.8$ Hz); 6.54 (s, 1H); 4.19 (t, 2H, $J = 4.2$ Hz); 1.77–1.71 (m, 2H); 1.50–1.41 (m, 2H); 0.99 (t, 3H, $J = 0.9$ Hz). ^{13}C NMR ($CDCl_3$, 100 MHz): 188.5, 163.4, 163.0, 136.6, 131.7, 131.2, 129.7, 128.5, 128.1, 125.7, 122.8, 97.7, 41.0, 30.5, 20.1, 13.1 ppm.

6 X-ray crystallography for 3

Crystals were grown as yellow prisms by slow evaporation from chloroform-d_3. The data were collected at −120 °C on a Nonius Kappa CCD diffractometer using a Bruker AXS Apex II detector and a graphite monochromator with MoKα radiation (λ = 0.71075 Å). Reduced temperatures were maintained by use of an Oxford Cryosystems 600 low-temperature device. A total of 2194 frames of data were collected using ω-scans with a scan range of 0.9° and a counting time of 62 seconds per frame. Details of crystal data, data collection and structure refinement are listed in Table S1.†

Acknowledgements

This work was supported by the U.S. National Science Foundation (CHE-1057904; J.L.S.), the Robert A. Welch Foundation (F-1018 to J.L.S.) and by a CRI project grant from National Research Foundation of Korea (NRF) grant funded by the Korea government (MSIP) (no. 2009-0081566; J.S.K.).

Notes and references

1 (*a*) P. T. Anastas, *Crit. Rev. Anal. Chem.*, 1999, **29**, 167; (*b*) P. T. Anastas and J. C. Warner, *Green Chemistry: Theory and Practice*, Oxford University Press, New York, 1998; (*c*) J. Buffle and G. Horvai, *In Situ Monitoring of Aquatic Systems: Chemical Analysis and Speciation*, Wiley, New York, 2001.

2 (*a*) P. D. Beer and P. A. Gale, *Angew. Chem., Int. Ed.*, 2001, **40**, 486; (*b*) S. K. Kim and J. L. Sessler, *Chem. Soc. Rev.*, 2010, **39**, 3784.

3 (*a*) H. N. Kim, W. X. Ren, J. S. Kim and J. Yoon, *Chem. Soc. Rev.*, 2012, **41**, 3210; (*b*) D. T. Quang and J. S. Kim, *Chem. Rev.*, 2010, **110**, 6280; (*c*) D.-G. Cho and J. L. Sessler, *Chem. Soc. Rev.*, 2009, **38**, 1647.

4 (*a*) X. Chen, G. Zhou, X. Peng and J. Yoon, *Chem. Soc. Rev.*, 2012, **41**, 4610; (*b*) Y. Zhou and J. Yoon, *Chem. Soc. Rev.*, 2012, **41**, 52; (*c*) Y. Zhou, Z. Xu and J. Yoon, *Chem. Soc. Rev.*, 2011, **40**, 2222.

5 (*a*) E. W. Schmidt, *Hydrazine and its Derivatives: Preparation, Properties, Applications*, Wiley, New York, 1984; (*b*) H. W. Schiessl, *Encyclopedia of Chemical Technology*, ed. K. Othmer, Wiley, New York, 3rd edn, 1980, 12, p. 734; (*c*) K. Yamada, K. Yasuda, N. Fujiwara, Z. Siroma, H. Tanaka, Y. Miyazaki and T. Kobayashi, *Electrochem. Commun.*, 2003, **5**, 892.

6 Y.-Y. Liu, I. Schmeltz and D. Hoffmann, *Anal. Chem.*, 1974, **46**, 885.

7 (*a*) J.-W. Mo, B. Ogorevc, X. Zhang and B. Pihlar, *Electroanalysis*, 2000, **12**, 48; (*b*) S. D. Zelnick, D. R. Mattie and P. C. Stepaniak, *Aviat., Space Environ. Med.*, 2003, **74**, 1285; (*c*) U. Ragnarsson, *Chem. Soc. Rev.*, 2001, **30**, 205; (*d*) V. Andries and D. Couturier, *Mater. Perform.*, 2000, **39**, 58.

8 M. Strous and M. S. M. Jetten, *Annu. Rev. Microbiol.*, 2004, **58**, 99.

9 (*a*) B. Toth, *Cancer Res.*, 1975, **35**, 3693; (*b*) S. Garrod, M. E. Bollard, A. W. Nicholls, S. C. Connor, J. Connelly, J. K. Nicholson and E. Holmes, *Chem. Res. Toxicol.*, 2005, **18**, 115; (*c*) C. A. Reilly and S. D. Aust, *Chem. Res. Toxicol.*, 1997, **10**, 328.

10 U.S. Environmental Protection Agency (EPA), *Integrated Risk Information System (IRIS) on Hydrazine/Hydrazine Sulfate. National Center for Environmental Assessment*, Office of Research and Development, Washington, DC, 1999.

11 J.-A. Oh, J.-H. Park and H.-S. Shin, *Anal. Chim. Acta*, 2013, **769**, 79.

12 Z. K. He, B. Fuhrmann and U. Spohn, *Anal. Chim. Acta*, 2000, **409**, 83.

13 (*a*) A. Umar, M. M. Rahman, S. H. Kim and Y.-B. Hahn, *Chem. Commun.*, 2008, 166; (*b*) J. Liu, Y. Li, J. Jiang and X. Huang, *Dalton Trans.*, 2010, **39**, 8693.

14 S. W. Thomas and T. M. Swager, *Adv. Mater.*, 2006, **18**, 1047.

15 (*a*) M. G. Choi, J. Hwang, J. O. Moon, J. Sung and S.-K. Chang, *Org. Lett.*, 2011, **13**, 5260; (*b*) M. G. Choi, J. O. Moon, J. Bae, J. W. Lee and S.-K. Chang, *Org. Biomol. Chem.*, 2013, **11**, 2961.

16 J. Fan, W. Sun, M. Hu, J. Cao, G. Cheng, H. Dong, K. Song, Y. Liu, S. Sun and X. Peng, *Chem. Commun.*, 2012, **48**, 8117.

17 X. Chen, Y. Xiang, Z. Li and A. Tong, *Anal. Chim. Acta*, 2008, **625**, 41.

18 W. Zhu, R. Yao and H. Tian, *Dyes Pigm.*, 2002, **54**, 147.

19 (*a*) Y. Kinoshita, M. Kunieda, Y. Mikata and H. Tamiaki, *Tetrahedron Lett.*, 2013, **54**, 1243; (*b*) J. C. Sloop, C. L. Bumgardner, G. Washington, W. D. Loehle, S. S. Sankar and A. B. Lewis, *J. Fluorine Chem.*, 2006, **127**, 780.

20 G. A. Crosby and J. N. Demas, *J. Phys. Chem.*, 1971, **75**, 991.

21 Z. Muňoz, A. S. Cohen, L. M. Nguyen, T. A. McIntosh and P. E. Hoggard, *Photochem. Photobiol. Sci.*, 2008, **7**, 337.

